IEEE Access
Multidisciplinary ⋮ Rapid Review ⋮ Open Access Journal

Received December 23, 2020, accepted December 28, 2020, date of publication January 4, 2021, date of current version January 13, 2021.

Digital Object Identifier 10.1109/ACCESS.2020.3049010

Influence of the Nonlinear Stiffness Parameter of the Vibratory Stress Relief Device on Strong Nonlinear Superharmonic Resonance

LIFANG ZHAO, RONGXIAN MO, YANZHOU LI, AND GANWEI CAI
College of Mechanical Engineering, Guangxi University, Nanning 530004, China

Corresponding author: Yanzhou Li (lyz197916@126.com)

This work was supported in part by the National Natural Science Foundation of China under Grant 51765005, in part by the Natural Science Foundation of Guangxi, China, under Grant 2019GXNSFAA245020, and in part by the Major Project of Science and Technology of Guangxi, China, under Grant guike AA19254021.

ABSTRACT Nonlinear superharmonic vibratory stress relief (VSR) is an effective way to solve the resonance problem of a high stiffness workpiece. However, strong nonlinear factors are present, and superharmonic resonance is relatively complicated when the entire device is a strongly nonlinear system. Choosing the best nonlinear stiffness parameter of the spring to allow the superharmonic resonance to generate a sufficient amplitude and sufficient dynamic stress becomes difficult. To solve this problem, it is necessary to explore the effect of the stiffness parameter on the system resonance: First, the nonlinear vibration situation of the VSR device is analysed, and the effect of the stiffness parameter on the vibration characteristics is explored under the action of the strong nonlinear system. Then, a simulated vibration table is used to verify the rule that the stiffness parameters affect the superharmonic resonance. It was shown that strong nonlinear theory provides a theoretical basis for simulating vibration table experiments, and the relationship between the spring stiffness parameter and amplitude satisfies a certain relationship, which provides a useful reference for the application and research of the VSR device for nonlinear superharmonic resonance.

INDEX TERMS Nonlinear superharmonic resonance, stiffness parameter, strongly nonlinear system.

I. INTRODUCTION

Eliminating the residual stress of components in the process of manufacturing is an important goal in the field of mechanical manufacturing. Vibratory stress relief (VSR) has drawn attention because of its advantages of no pollution, high efficiency, time saving, energy saving and cost saving [1]. VSR was first discovered by American scientist J.W. Sratt [2] at the beginning of the 20th century and many results [3]–[6] have been obtained so far. Among them, the principle of VSR was proposed by the Wozney & Crawmer criterion [7]: ''when the sum of the dynamic stress in VSR and residual stress is greater than the yield limit of the materials and is less than the fatigue limit of the materials, the residual stress will be relaxed and released'', which is considered to be the most important VSR condition. However, the scope of application is still very limited. There is still substantial potential for VSR applications that has not been utilized. The main reason is that the excitation frequency produced by the current exciter cannot approach or reach the natural frequency of the workpiece with high stiffness. Therefore, the residual stress of the workpiece with high stiffness cannot be reduced [8].

Many researchers have studied the methods of serial connection and frequency reduction of workpieces, vibration table methods, etc. to solve these problems. With these methods, it is difficult to achieve the expected results because they cannot change the stiffness of workpieces themselves and the excitation frequency of the exciter is still much lower than the natural frequency of the high stiffness workpiece. It is difficult for the workpiece to produce enough elastic deformation resonance to reduce the residual stress.

In recent years, many researchers have filled the gap in this area and have proved the rationality and effectiveness in reducing residual stress mechanisms and experimental application. Abdullah *et al.* [9] introduced ultrasonic vibratory

The associate editor coordinating the review of this manuscript and approving it for publication was Hassen Ouakad.

stress relief (UVSR), the core of which is to use ultrasonic transducers to obtain a high excitation frequency and excite the component. This is unlikely to cause fatigue damage to components. However, Abdullah *et al.* [10] also pointed out that it is necessary to greatly increase the intensity of ultrasonic waves to obtain a higher excitation frequency, which puts forward higher requirements for the design of ultrasonic transducers. Wang and He [11], He *et al.* [12] proposed high frequency vibratory stress relief, which refers to high frequency resonance signals with frequency greater than 1 kHz that excite a small part of the workpiece. Local microscopic resonance occurs in a small area of the workpiece. High frequency VSR is suitable for local treatment of welds, etc., but it is difficult to use for stress relief of the overall structure.

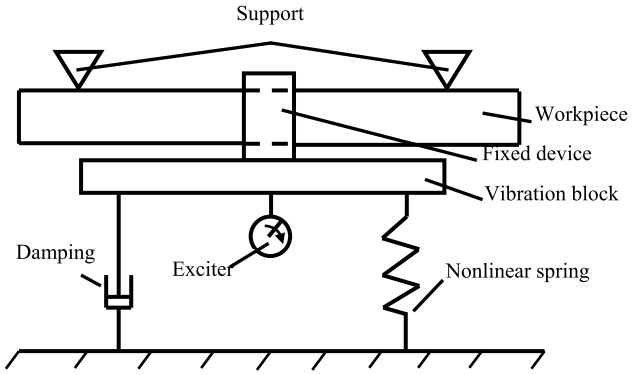

FIGURE 1. Schematic diagram of the nonlinear superharmonic resonance system.

The VSR device uses superharmonic resonance characteristics to eliminate residual stress on workpieces with high stiffness. The system schematic diagram is shown in Fig. 1, where the excitation force is generated by the inertial exciter (the inertial exciter composed of the current excitation motor and its eccentric device) and acts on the excitation block. When the parameter setting is appropriate, the excitation block generates superharmonic resonance under the combined action of a damper and nonlinear spring. The resonance is transmitted to the workpiece by the excitation block, so that the workpiece can obtain high frequency excitation which exceeds the excitation frequency of the inertial exciter [13].

According to the Wozney & Crawmer criterion of VSR, the residual stress of the workpiece is required to have sufficient elastic deformation, so the system needs to reach a certain amplitude.

To obtain a large output amplitude under the same input situation, it is often necessary to show strong nonlinear characteristics by attaching springs. Strong nonlinear systems have more complex dynamics for scholars to explore compared with weak nonlinear systems [14]–[18].

In reference [19], the mechanism analysis of the VSR device of nonlinear superharmonic resonance has been explored. A brief introduction is presented as follows: the workpiece generates elastic deformation under the action of the VSR device to obtain sufficient dynamic stress, introduces local micro plastic deformation at the residual stress of the

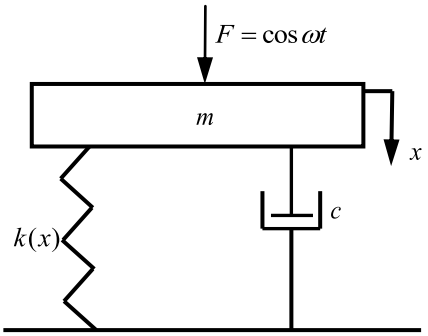

FIGURE 2. Single-degree-of-freedom nonlinear vibration system.

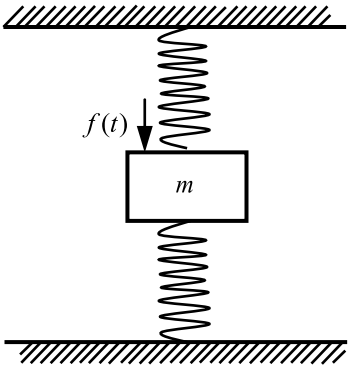

FIGURE 3. Nonlinear vibration system with workpiece with a single degree of freedom.

workpiece, and reduces residual stress. The workpiece has the characteristics of both mass and elastic elements in the process of VSR. For convenience, Fig. 2 is simplified as a mass spring model in Fig. 3. The differential equation of motion can be written using Newton's second law:

$$m\frac{d^2x}{dt^2} + c\frac{dx}{dt} + f(x) + k_q x = F\cos\omega t \tag{1}$$

where m is the equivalent mass of the excitation block, workpiece, etc. The external excitation force is $F\cos\omega t$, the displacement of the excitation block and workpiece is x, and the damping coefficient is c. The restoring force of the nonlinear and equivalent springs are $f(x)$ and $k_q x$. Since the n-th power term of the nonlinear term determines the order of superharmonic resonance of the system [20]. If there is a second and third nonlinear restoring force in the system, the system can generate second and third superharmonic resonance.

It is evident from the references [13], [19] that the VSR device for nonlinear superharmonic resonance has been analysed with working mechanisms and preliminary experimental research. However, for nonlinear the VSR system, the nonlinear restoring force is the key factor to produce superharmonic resonance, and the stiffness coefficient of the nonlinear spring has a great influence on the amplitude of superharmonic resonance. The above references do not provide sufficient information for the analysis of the stiffness of the nonlinear spring in the system. In this paper, the influence of the nonlinear stiffness on the VSR device is studied: firstly, according

to the differential equations of the system motion, the strong and weak nonlinear vibrations are analysed, and the response of the stiffness coefficient to the superharmonic resonance under the action of the strong nonlinear system is studied. Then, the simulated vibration table is used to verify the rule that the stiffness parameters affect superharmonic resonance, which provides the basis for the application of VSR technology.

II. SYSTEM ANALYSIS

A. SOLVING THE NONLINEAR SYSTEM EQUATIONS

In the studies of nonlinear vibration, the difference between the calculation methods for strong and weak nonlinear systems is that the nonlinear term in the system cannot be regarded as containing small parameters, and the nonlinear part cannot be regarded as a perturbation of the linear part. In the strong nonlinear method, the modified L-P method transforms the large parameter into the small parameter through parameter transformation, and then the weak nonlinear L-P method is applied. It is easy to compare two different nonlinear methods. These two methods are used to analyse the weak and strong nonlinear response characteristics of nonlinear VSR systems. The influence of different nonlinear stiffness parameters on superharmonic resonance is explored. The nonlinear vibration system is simplified as shown in Fig. 2 to obtain Fig. 3.

The mass of the object is set to $m = m_1 + m_2 + m_q$, and the mass of the exciter block, the mass of the exciter and the equivalent mass of the component are m_1, m_2 and m_q, respectively. The upper-end spring stiffness and the lower end spring stiffness are k_1 and k_2. The differential equation of motion of an object is as follows:

$$\ddot{x} + 2\varepsilon\mu\dot{x} + \omega_0^2 x - \varepsilon k_3 x^3 = p\cos\omega t \tag{2}$$

where ω_0 is the natural frequency of the system, $\omega_0 = \sqrt{k_1/m}$, $\mu = 0$, $\varepsilon k_3 = k_2/m$, and $p = F/m$.

1) WEAK NONLINEAR CASE

When k_1 is greater than k_2 and ε is a small parameter, the system can be regarded as a cubic weak nonlinear system. At this time, the L-P method is used to solve the system. The response of the excitation force frequency is close to 1/n of the natural frequency of the system (n is a positive integer not equal to 1).

Assuming $\tau = \omega t + \theta$, $H = p\cos\theta$, and $K = p\sin\theta$, the purpose of introducing θ as the unknown phase angle is to conveniently set the initial conditions. Equation (2) is transformed into:

$$\omega^2 x'' + \omega_0^2 x = \varepsilon f(x, \omega x') + H\cos\tau + K\sin\tau \tag{3}$$

where $f(x, \omega x') = k_3 x^3$, x' represents the x partial derivative of τ, and ε is a small parameter

x is expanded into a power function of ε, ω can be represented by an expansion having the form of (5):

$$x = x_0(\tau) + \varepsilon x_1(\tau) + \varepsilon^2 x_2(\tau) + \cdots \tag{4}$$

$$\omega = \frac{1}{n}\omega_0(\tau) + \varepsilon\omega_1(\tau) + \varepsilon^2\omega_2(\tau) + \cdots \tag{5}$$

Substituting (4) and (5) into (3) and omitting the terms above for ε^2 gives:

$$\begin{aligned}&(1 + 2\varepsilon n\frac{\omega_1}{\omega_0} + \cdots)(x_0'' + \varepsilon x_1'' + \varepsilon^2 x_2'' + \cdots)\\ &\quad + n^2\left(x_0 + \varepsilon x_1 + + \varepsilon^2 x_2 + \cdots\right)\\ &= \frac{\varepsilon n^2}{\omega_0^2}k_3(x_0 + \varepsilon x_1 + \varepsilon^2 x_2 + \cdots)^3 + \frac{n^2}{\omega_0^2}(H\cos\tau + K\sin\tau)\end{aligned} \tag{6}$$

Equate the coefficients of ε:

$$x_0'' + n^2 x_0 = \frac{n^2}{\omega_0^2}(H\cos\tau + K\sin\tau) \tag{7}$$

$$x_1'' + n^2 x_1 = \frac{n^2}{\omega_0^2}\left(k_3 x_0^3 - \frac{2}{n}\omega_0\omega_1 x_0''\right) \tag{8}$$

The solution of (7) is:

$$x_0 = A\cos n\tau + B\sin n\tau + \Lambda_1\cos\tau + \Lambda_2\sin\tau \tag{9}$$

where $\Lambda_1 = \frac{n^2 H}{(n^2-1)\omega_0^2}$, $\Lambda_2 = \frac{n^2 K}{(n^2-1)\omega_0^2}$

When n = 3, by substituting (9) into (8), eliminating secular terms, and assuming the coefficient of $\cos 3\tau$ and $\sin 3\tau$ are 0, equation(8) can be written as follows after eliminating the secular terms:

$$\begin{aligned}x_1'' + 9x_1 = \frac{27k_3}{4\omega_0^2}\Big[&\left(2A^2\Lambda_1 + A\Lambda_1^2 - A\Lambda_2^2 + 2B^2\Lambda_1 + \Lambda_1^3\right.\\ &\left. + 2B\Lambda_1\Lambda_2 + \Lambda_1\Lambda_2^2\right)\cos\tau + \left(2A^2\Lambda_2 + B\Lambda_1^2\right.\\ &\left. - B\Lambda_2^2 + \Lambda_2^3 + 2B^2\Lambda_2 - 2A\Lambda_1\Lambda_2 + \Lambda_1^2\Lambda_2\right)\sin\tau\\ &+ \left(A^2\Lambda_1 + 2AB\Lambda_2 + A\Lambda_1^2 - A\Lambda_2^2 - B^2\Lambda_1\right.\\ &\left. - 2B\Lambda_1\Lambda_2\right)\cos 5\tau + (2AB\Lambda_1 - A^2\Lambda_2 + B\Lambda_1^2\\ &- B\Lambda_2^2 + B^2\Lambda_2 + 2A\Lambda_1\Lambda_2)\sin 5\tau\\ &+ \left(A^2\Lambda_1 - 2AB\Lambda_2 - B^2\Lambda_1\right)\cos 7\tau\\ &+ \left(A^2\Lambda_2 + 2AB\Lambda_1 - B^2\Lambda^2\right)\sin 7\tau\\ &+ H\cos\tau + K\sin\tau\end{aligned} \tag{10}$$

The solution to (10) can be solved for x_1, where the initial conditions are $x_0(0) = 0$, $\dot{x}_0(0) = 0$, $x_1(0) = 0$, and $\dot{x}_1(0) = 0$. The first-order approximate solution of (3) is

$$x_1 = x_0 + \varepsilon x_1 + O(\varepsilon^2) \tag{11}$$

where $\omega = \omega_0 + \varepsilon\omega_1 + O(\varepsilon^2)$

2) STRONG NONLINEAR CASE

When k_2 is greater than k_1 and ε is a large parameter, the system can be regarded as a cubic strong nonlinear system under forced vibration. At this time, the MLP method is used to solve the system [21].

Assuming $\tau = \omega t + \theta$, $H = p\cos\theta$, and $K = p\sin\theta$, equation (2) is transformed into:

$$\omega^2 x'' + \omega_0^2 x = \varepsilon f(x, \omega x') + H\cos\tau + K\sin\tau \tag{12}$$

where $f(x, \omega x') = k_3 x^3$, x' represents the x partial derivative of τ, and ε is a large parameter.

Considering the influence of the fundamental frequency harmonic response, ω^2 is expanded into a power function of ε

$$\omega^2 = \frac{1}{n^2}\omega_0^2(\tau) + \varepsilon\omega_1(\tau) + \varepsilon^2\omega_2(\tau) + \cdots \tag{13}$$

A transformation parameter is introduced as follows:

$$\alpha = \varepsilon\omega_1/(\frac{1}{n^2}\omega_0^2 + \varepsilon\omega_1) \tag{14}$$

thus

$$\omega^2 = \frac{1}{n^2}\frac{\omega_0^2}{(1-\alpha)}(1 + \delta_2\alpha^2 + \delta_3\alpha^3 + \cdots) \tag{15}$$

or

$$\omega = \frac{\omega_0}{n}\left[1 + \frac{1}{2}\alpha + (\frac{3}{8} + \frac{\delta_2}{2})\alpha^2 + \cdots\right] \tag{16}$$

x is expanded into a power function of α.

$$x = x_0(\tau) + \alpha x_1(\tau) + \alpha^2 x_2(\tau) + \cdots \tag{17}$$

Substituting (13) - (17) into (12) and omitting the terms above α^2 gives

$$\begin{aligned}(1 + \delta_2\alpha^2 + \delta_3\alpha^3 + \cdots)(x_0'' + \alpha x_1'' + \alpha^2 x_2'' + \cdots)\\ + n^2(1-\alpha)(x_0 + \alpha x_1 + \alpha^2 x_2 + \cdots)\\ = \frac{\alpha}{\omega_1}k_3(x_0 + \alpha x_1 + \alpha^2 x_2 + \cdots)^3\\ + \frac{n^2}{\omega_0^2}(1-\alpha)(H\cos\tau + K\sin\tau)\end{aligned} \tag{18}$$

Equate the coefficients of α. The all order perturbation can be obtained as:

$$x_0'' + n^2 x_0 = \frac{n^2}{\omega_0^2}(H\cos\tau + K\sin\tau) \tag{19}$$

$$x_1'' + n^2 x_1 = n^2 x_0 + \frac{1}{\omega_1}k_3 x_0^3 - \frac{n^2}{\omega_0^2}(H\cos\tau + K\sin\tau) \tag{20}$$

The solution of (19) is

$$x_0 = A\cos n\tau + B\sin n\tau + \Lambda_1\cos\tau + \Lambda_2\sin\tau \tag{21}$$

where $\Lambda_1 = \frac{n^2 H}{(n^2-1)\omega_0^2}$, $\Lambda_2 = \frac{n^2 K}{(n^2-1)\omega_0^2}$

When n = 3, equation (21) is substituted into (20) and the secular terms are eliminated. Assuming the coefficients of $\cos 3\tau$ and $\sin 3\tau$ are 0 gives:

$$\begin{aligned}9A + \frac{k_3}{4\omega_1}\left[3A\left(A^2 + B^2\right) + 6A\left(\Lambda_1^2 + \Lambda_2^2\right)\right.\\ \left. + \Lambda_1^3 - 3\Lambda_1\Lambda_2^2\right] = 0\\ 9B + \frac{k_3}{4\omega_1}\left[3B\left(A^2 + B^2\right) + 6B\left(\Lambda_1^2 + \Lambda_2^2\right)\right.\\ \left. - \Lambda_2^3 + 3\Lambda_1^2\Lambda_2\right] = 0\end{aligned} \tag{22}$$

Assuming $A^2 + B^2 = a^2$ and $M^2 = \Lambda_1^2 + \Lambda_2^2 = 81p^2/64\omega_0^4$, the amplitude-frequency equation can be written as follows:

$$\begin{aligned}\left(\frac{9k_3^2}{16\omega_1^2}\right)a^6 + \left(\frac{9k_3^2}{4\omega_1^2}M^2 + \frac{27k_3}{2\omega_1}\right)a^4\\ + \left(81 + \frac{9k_3^2}{4\omega_1^2}M^4 + \frac{27k_3}{\omega_1}M^2\right)a^2 - \frac{k_3^2 M^6}{16\omega_1^2} = 0\end{aligned} \tag{23}$$

Solving (20) after eliminating the secular terms gives:

$$\begin{aligned}x_1 = C_1\cos 3\tau + C_2\sin 3\tau + \frac{9}{8}(\Lambda_1\cos\tau + \Lambda_2\sin\tau)\\ + \frac{3k_3}{32\omega}\left[\left(2A^2\Lambda_1 + A\Lambda_1^2 - A\Lambda_2^2 + 2B^2\Lambda_1 + 2B\Lambda_1\Lambda_2\right.\right.\\ \left. + \Lambda_1^3 + \Lambda_1\Lambda_2^2\right)\cos\tau + \left(2A^2\Lambda_2 + B\Lambda_1^2 - B\Lambda_2^2 + \Lambda_2^3\right.\\ \left. + 2B^2\Lambda_2 - 2A\Lambda_1\Lambda_2 + \Lambda_1^2\Lambda_2\right)\sin\tau - \frac{1}{2}(2AB\Lambda_2\\ + A^2\Lambda_1 + A\Lambda_2^2 - 2B\Lambda_1\Lambda_2 - A\Lambda_2^2 - B^2\Lambda_1)\cos 5\tau\\ - \frac{1}{2}\left(2AB\Lambda_1 - A^2\Lambda_2 + 2A\Lambda_1\Lambda_2 + B\Lambda_1^2 - B\Lambda_2^2 + B^2\Lambda_2\right)\\ \times\sin 5\tau - \frac{1}{5}\left(A^2\Lambda_1 - 2AB\Lambda_2 - B^2\Lambda_1\right)\cos 7\tau\\ - \frac{1}{5}\left(A^2\Lambda_2 + 2AB\Lambda_1 - B^2\Lambda_2\right)\sin 7\tau\Big]\\ - \frac{9}{8\omega_0^2}(H\cos\tau + K\sin\tau)\end{aligned} \tag{24}$$

where C_1 and C_2 are undetermined coefficients, and the initial conditions are $x_0(0) = 0$, $\dot{x}_0(0) = 0$, $x_1(0) = 0$, and $\dot{x}_1(0) = 0$. The first- order approximate solution of (3) is

$$x_1 = x_0 + \alpha x_1 + O(\varepsilon^2) \tag{25}$$

where $\omega^2 = \frac{1}{n^2}\frac{\omega_0^2}{(1-\alpha)}[1 + O(\alpha)]$

Based on the results above, numerical calculations and qualitative analyses are performed on weak and strong nonlinear systems, and the cubic stiffness parameters of the strong nonlinear system are analysed. When the excitation frequency is 1/3 of the natural frequency, the system will generate superharmonic resonance.

Assume that $\omega_0 = 3rad/s$, $\omega = 1rad/s$ and $F = 5N$ The system can be regarded as a weak nonlinear system when $k_1 = 9N/mm$ and $k_2 = 1N/mm$. When $k_1 = 9N/mm$ and $k_2 = 10, 20$ and $30N/mm$, the system can be regarded as a cubic strong nonlinear system under forced vibration. The first-order approximate solution is solved.

In Fig. 4, the first-order approximate solutions are different. Although the difference in the k_2 coefficients is 10 times and the other parameters are the same, the amplitude value of the solution of the strong nonlinear system is 13.857 times that of the weak nonlinear system. When the strong nonlinear system vibrates, the curves show that the maximum amplitude of the first-order approximate solution of x increases with the increase in the cubic term coefficient in Fig. 4. A larger resonance amplitude can be obtained from a smaller excitation amplitude for strong nonlinear resonance, which

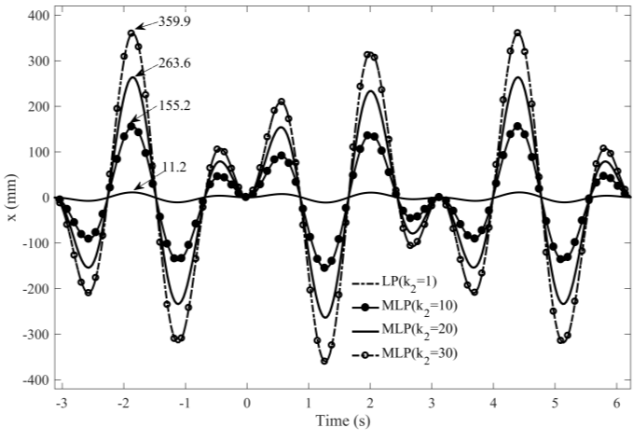

FIGURE 4. First-order approximate solutions.

provides a theoretical basis for the design of the VSR device for nonlinear superharmonic resonance.

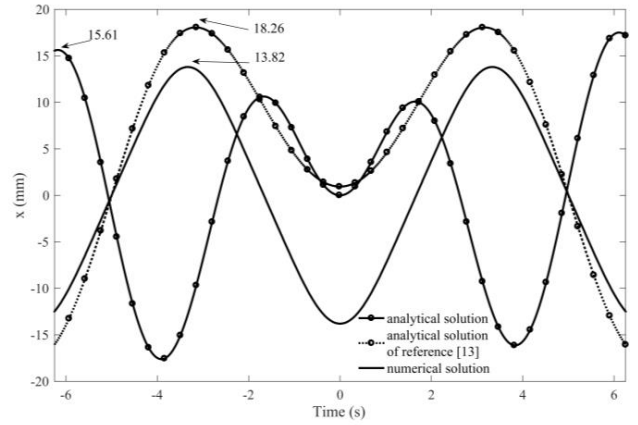

FIGURE 5. Comparison of the first-order approximate solutions.

Compared with the strong nonlinear calculation method used in reference [13], the same parameters are used for the calculation and numerical solution [22], as shown in Fig. 5. It can be found that the result of the method used in this paper is close to the numerical solution and has high accuracy.

B. FREQUENCY AMPLITUDE RESPONSE ANALYSIS OF THE STIFFNESS PARAMETERS

The influence of stiffness parameters on system resonance is analysed according to the amplitude-frequency equation. As shown in Fig. 6, when the cubic term coefficient increases gradually, the frequency curve of the third harmonic response moves to the right, the amplitude of the resonance point and the region of superharmonic resonance also increase, and the amplitude-frequency curve exhibits a jumping phenomenon. Setting the same parameters above and taking different stiffness coefficient values, the maximum value of the amplitude is determined (the value of the highest point in Fig. 6), as shown as the '$*$' in Fig. 7. Due to the different excitation force frequencies, excitation force amplitudes and damping

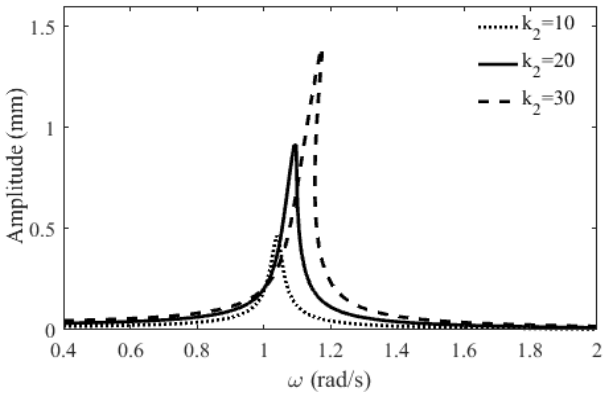

FIGURE 6. Analysis of the frequency amplitude response of the strong nonlinear system.

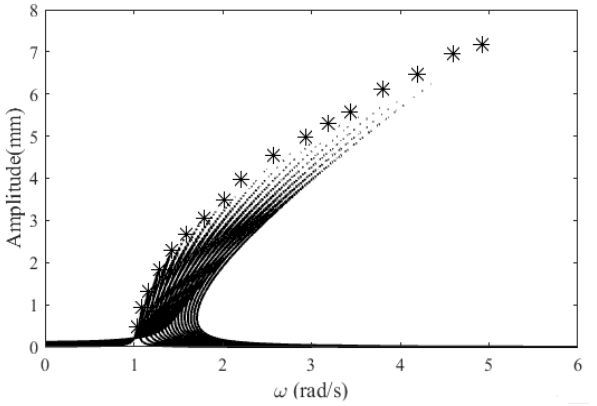

FIGURE 7. Frequency response analysis of different stiffness systems.

used in practice, the response amplitude is also different. Therefore, the different stiffness coefficients and amplitudes are used as variables. Through data fitting, it is found that the relationship between the nonlinear stiffness parameters and amplitude satisfies as the following:

$$\Delta a \approx 0.47\eta\Delta k \tag{26}$$

where Δk_3 is the difference between the two stiffness coefficients, Δa is the increased amplitude value caused by Δk_3, and η is the error coefficient due to different excitation force frequencies and damping.

III. EXPERIMENT

To further explore the influence of the nonlinear stiffness coefficient on the system, the relationship between the nonlinear parameters and amplitude is verified by an experiment. The experimental equipment include a DZST-3B multi-function combination test-bed, Microcomputer controlled electronic universal testing machine of WDW type, JZK-2 exciter and SHX2112 VSR instrument. The test vibration signal is collected by a Jingnan data acquisition instrument. The main hardware includes a MDR mobile data recorder, 608A11/M010AC acceleration sensor, and notebook computer; the software includes mobile data acquisition software and DDP spectrum analysis software.

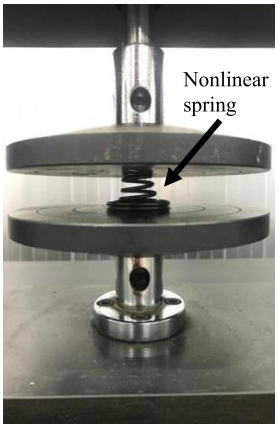

FIGURE 8. Compression test of cylindrical spiral springs.

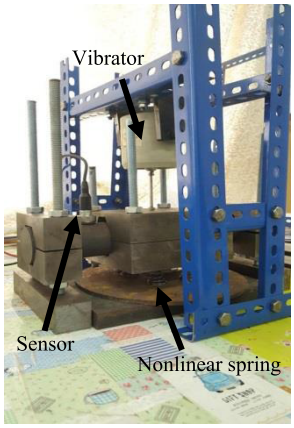

FIGURE 9. Simulated vibration table.

A. METHOD

Three groups of cylindrical spiral springs with different parameters are selected, and the spring compression test (as shown in Fig. 8) and origin software are used to fit the curves to obtain the characteristic spring equation with different stiffness coefficients. A cylindrical workpiece with a diameter of 50 mm is selected as the object and the acceleration sensor is installed on the cylinder close to the excitation block. Considering the accuracy of the data, the electromagnetic vibrator is installed upside down on the cylinder and the excitation force acts on the cylinder through the clamp block, as shown in Fig. 9. The excitation force and frequency output from the electromagnetic exciter is controlled by the signal generator. During the experiment, the excitation voltage of each spring vibration process is maintained by the signal generator. The recorder collects the vibration signals of the supporting cylinders of each group of springs with three resonance response signals and the average value of the data.

B. RESULTS AND DISCUSSION

The analysis results of the experiment are shown in Table 1. In practice, the characteristic equation of the fitted spring equation contains square and cubic terms, and a spring with similar linear and square terms as those in the characteristic equation are selected to ensure the accuracy of the cubic

TABLE 1. Experiments of springs with different cubic stiffness coefficients.

Springs	1	2	3
Linear term (N/mm)	15.068	15.261	15.970
Square term (N/mm)	-13.030	-13.325	-13.868
Cubic term (N/mm)	4.394	5.804	6.504
Amplitude of 20 Hz (mm)	0.875	0.912	0.976
Amplitude of 40 Hz (mm)	0.586	0.611	0.677
Amplitude of 60 Hz (mm)	0.302	0.369	0.403

stiffness parameter experiment. Three groups of springs with different cubic term stiffness parameters with second and third harmonic responses on the cylinder at an excitation frequency of 20 Hz are shown in Fig. 10 to Fig. 12. It is found that the workpiece has achieved superharmonic resonance under the experiment, and the VSR treatment of the high stiffness workpiece can be realized under the condition of reasonably selecting the parameters.

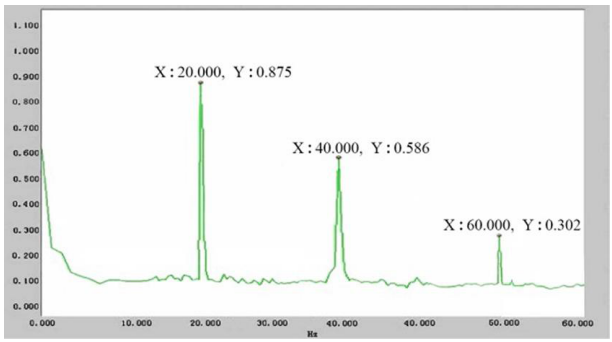

FIGURE 10. Results of spring No. 1.

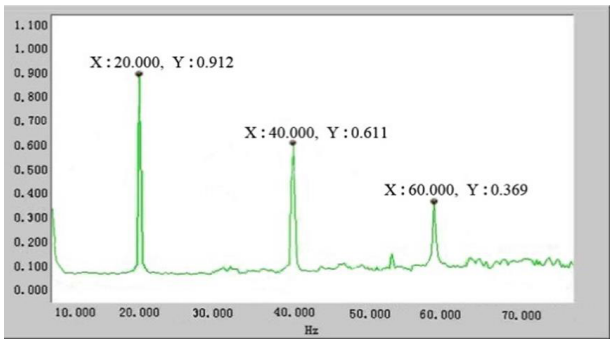

FIGURE 11. Results of spring No. 2.

Through the analysis with an amplitude of 60 Hz, with the increase in the cubic term of the spring equation, the amplitude increases gradually, and the occurrence of the third harmonic resonance becomes more obvious. The experiment values of 3 groups of different parameters of the spring meet (26) under the condition of allowable error by setting $\eta = 0.1$ and calculating the amplitude of three times the frequency.

To prove the application in practice, the response amplitude of the superharmonic resonance required of the workpiece is assumed to be 0.43 mm - 0.68 mm. Therefore, a spring with

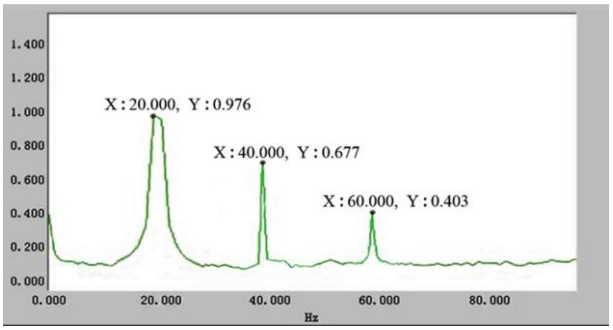

FIGURE 12. Results of spring No. 3.

a cubic term stiffness parameter of 8.236 N/mm is selected for the experiment, and the response is shown in Fig. 13. The three times response amplitude is 0.483 mm, which meets the requirements.

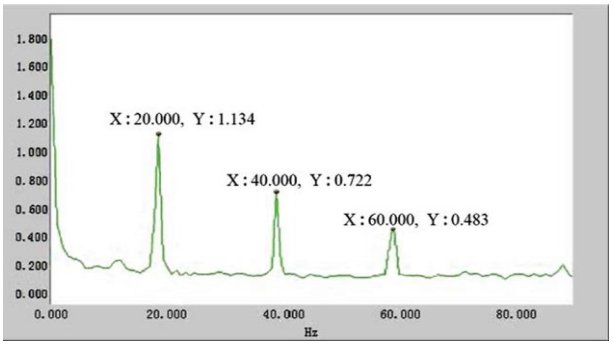

FIGURE 13. Experimental results of nonlinear superharmonic resonance.

The analysis above proves the correctness of the theoretical analysis. When designing the VSR device for nonlinear superharmonic resonance, the higher the nonlinear coefficient of the nonlinear spring used by the platform, the more helpful it is to excite the nonlinear resonance at a higher frequency. The high stiffness workpiece can obtain a sufficiently large dynamic stress for larger amplitude resonance, which meets the requirement for eliminating residual stress. A suitable spring can be quickly obtained through the relationship between the stiffness parameters and amplitude according to the required amplitude.

IV. CONCLUSION

This paper studies the VSR device for nonlinear superharmonic resonance. System analyses and simulated vibration table experiments are applied. The most important results of this research are summarized as follows:

(1) When the VSR device is in strong nonlinear vibration, the strong nonlinear quantitative method (modified LP method) has higher accuracy than other methods. This proves that a large resonance amplitude can be obtained with a small excitation amplitude which provides a basis for the application of the superharmonic VSR device;

(2) With the increase in the stiffness parameters of the cubic term of the nonlinear spring, the superharmonic resonance amplitude increases gradually and satisfies a certain relational expression, which is demonstrated in the experiment;

(3) According to the amplitude conditions required by the high stiffness workpiece, a suitable spring can be quickly selected based on the relationship between the nonlinear stiffness parameter and the amplitude, which can save time. The results also can be applied to common strong nonlinear systems;

(4) A device with a cubic nonlinear spring can result in the large frequency range of the superharmonic response. Excitation near the true fraction of the natural frequency of the system may also obtain a more obvious superharmonic resonance response, and it is greatly affected by the coefficient of the nonlinear term. The reasons and rules for this behaviour need to be further studied.

The above conclusions prove the correctness and application feasibility of the theory of the nonlinear superharmonic resonance platform of high stiffness workpieces and provide an effective method for solving the problem that VSR cannot eliminate the residual stress of high stiffness workpieces.

REFERENCES

[1] H. Gao, Y. Zhang, Q. Wu, J. Song, and K. Wen, "Fatigue life of 7075-T651 aluminium alloy treated with vibratory stress relief," *Int. J. Fatigue*, vol. 108, pp. 62–67, Mar. 2018.

[2] C. Z. Liu, X. M. Yang, H. S. Zhou, Q. Gao, and X. U. Xiao-Fang, "Review of vibration stress relief technology," *Tech. Acoust.*, vol. 36, no. 1, pp. 42–49, 2017.

[3] T. Lv and Y. Zhang, "Dynamic stress analysis for vibratory stress relief through the vibration platform," in *Proc. IEEE Workshop Electron., Comput. Appl.*, May 2014, pp. 560–563.

[4] C. Nicola, A. Vintila, M. Nicola, V. Voicu, M. C. Nitu, and M. Duta, "System and method for controlled vibration stress relief of metal parts with residual internal stresses," in *Proc. Int. Conf. Appl. Theor. Electr. (ICATE)*, Oct. 2016, pp. 1–4.

[5] S. Mohanty, M. Arivarasu, N. Arivazhagan, and K. V. P. Prabhakar, "The residual stress distribution of CO_2 laser beam welded AISI 316 austenitic stainless steel and the effect of vibratory stress relief," *Mater. Sci. Eng., A*, vol. 703, pp. 227–235, Aug. 2017.

[6] S. Y. Kasim and N. S. Abttan, "Experimental comparison study on stress relief for welded low carbon steel (St 37) bar by vibration mechanism and heat treatment process," in *Proc. IPO Conf. Mater. Eng. Sci.*, vol. 454, 2018, Art. no. 012121.

[7] G. P. Wozney and G. R. Crawmer, "An investigation of vibrational stress relief in steel," *Weld. J.*, vol. 47, no. 9, pp. 411–419, 1968.

[8] G. W. Cai, P. Deng, Y. C. Pan, H. Z. Wang, and L. Zhang, *Present Situation and Countermeasures of Vibratory Stress Relief Technology*, vols. 151–156. Beijing, China: China Machine Press, 2011.

[9] A. Abdullah, M. Malaki, and A. Eskandari, "Strength enhancement of the welded structures by ultrasonic peening," *Mater. Des.*, vol. 38, pp. 7–18, Jun. 2012.

[10] M. Shalvandi, Y. Hojjat, A. Abdullah, and H. Asadi, "Influence of ultrasonic stress relief on stainless steel 316 specimens: A comparison with thermal stress relief," *Mater. Des.*, vol. 46, pp. 713–723, Apr. 2013.

[11] J. W. Wang and W. He, "Research on the technology of high frequency vibratory stress relief," *Mach. Tool Hydraul.*, vol. 9, pp. 9–11 and 94, Oct. 2005.

[12] W. He, X.-Y. Cheng, and R.-J. Shen, "Research on high-frequency vibratory stress relief for small assembly," in *Proc. 1st IEEE Int. Conf. Nano/Micro Engineered Mol. Syst.*, Jan. 2006, p. 1428.

[13] G. W. Cai, Y. Z. Li, Y. X. Huang, and R. G. Wang, *Study on Vibratory Stress Relief Devices of Nonlinear Resonance and Coupled Resonance*. Wuhan, China: Wuhan Univ. Technol. Press, 2018.

[14] D. Shao, Z. Q. Lu, and L. Q. Chen, "Power flow characteristics of a two-stage nonlinear vibration isolation system," *J. Vibrat. Eng.*, vol. 30, no. 5, pp. 764–773, 2017.

[15] C. Zhao, G. Sobreviela, M. Pandit, S. Du, X. Zou, and A. Seshia, "Experimental observation of noise reduction in weakly coupled nonlinear MEMS resonators," *J. Microelectromech. Syst.*, vol. 26, no. 6, pp. 1196–1203, Dec. 2017.
[16] W. P. Sun and C. W. Lim, "A generalization of Lindstedt–Poincaré perturbation method to strongly mixed-parity nonlinear oscillators," *IEEE Access*, vol. 8, pp. 214894–214901, 2020.
[17] Y. D. Hu and H. J. Bao, "Strongly nonlinear natural vibration of the functionally graded rotating circular plate in the thermal environment," *Chin. J. Solid Mech.*, vol. 41, no. 4, pp. 258–272, 2020.
[18] Z. Y. Tian, W. J. Song, and X. X. Wang, "Application of improved multiscale method in static wind stability analysis of membrane roof," *Building Sci.*, vol. 36, no. 3, pp. 10–16, 2020.
[19] G. W. Cai, P. Deng, Y. Z. Li, and Y. X. Huang, "Research on the mechanisms of the novel VSR devices with nonlinear superharmonic vibration," *J. Vib., Meas. Diagnosis*, vol. 33, no. 2, pp. 105–108 and 222, 2013.
[20] R. S. Chen, *Nonlinear Vibration*. Beijing, China: Higher Education Press,2002.
[21] Z. Q. Li and Z. A. Yang, "Strong nonlinear primary resonance analysis of end-shield with motor," *J. Mech. Strength*, vol. 37, no. 2, pp. 368–372, 2015.
[22] S. Stoyanov, "Analytical and numerical investigation on the duffing oscilator subjected to a polyharmonic force excitation," *J. Theor. Appl. Mech.*, vol. 45, no. 1, pp. 3–16, Mar. 2015.

LIFANG ZHAO is currently pursuing the master's degree with the College of Mechanical Engineering, Guangxi University, Nanning, China. Her current research interest includes dynamics of machinery.

RONGXIAN MO is currently pursuing the master's degree with the College of Mechanical Engineering, Guangxi University, Nanning, China. His current research interest includes dynamics of machinery.

YANZHOU LI received the Ph.D. degree from the College of Civil Engineering, Guangxi University, Nanning, China, in 2013. He is currently an Associate Professor with the College of Mechanical Engineering, Guangxi University. His research interest includes mechanical vibration and control.

GANWEI CAI received the Ph.D. degree from the College of Mechanical Engineering, Huazhong University of Science and Technology, Wuhan, China, in 1998. He is currently a Professor with the College of Mechanical Engineering, Guangxi University, Nanning, China. His current research interests include dynamics of machinery and MDOF controllable mechanisms.